EXPERIMENTAL INVESTIGATION AND PERFORMANCE PREDICTION OF CRYOGENIC TEMPERATURE SENSOR FOR CRYOGENIC ROCKET ENGINE USING ARTIFICIAL INTELLIGENCE TECHNIQUES

Poster # 399

Upendra Behera[1*], Debashis Panda[1], Chandrasekharan C[2], Jeen Britto M[2], Cross Sapna A[2] and D.S. Nadig[1]

[1] Centre for Cryogenic Technology, Indian Institute of Science, Bangalore, India

[2] ISRO Propulsion Complex, Indian Space Research Organization, Mahendragiri, India

ICEC/ICMC
29th International Cryogenic Engineering Conference
International Cryogenic Materials Conference 2024
July 22-26, 2024, Geneva, Switzerland

MOTIVATION

- Temperature measurement is essential for smooth and reliable functioning of cryogenic & semicryogenic rocket engines.
- Highly accurate, reliable and robust sensors have been in-house developed and used for temperature measurement.
- Calibration of sensors is essential in regular intervals to measure the repeatability of sensor.
- Polynomial fittings are mostly used to establish relation between resistance and temperature for intermediate measuring points.
- Neural network method has been used to establish relationship between resistance and temperature for the first time.
- Different types of backpropagation schemes are chosen to identify the best one.

ISRO'S CRYOGENIC ROCKET ENGINE

Rocket engine consists of propellant and fuel tanks, a convergent-divergent nozzle, a combustion chamber, turbo machineries, and other accessories to feed the fuel and oxidizer from storage tanks to combustion chamber [1].

Anatomy of ISRO's cryogenic rocket engine

EXPERIMENTAL TEST RIG

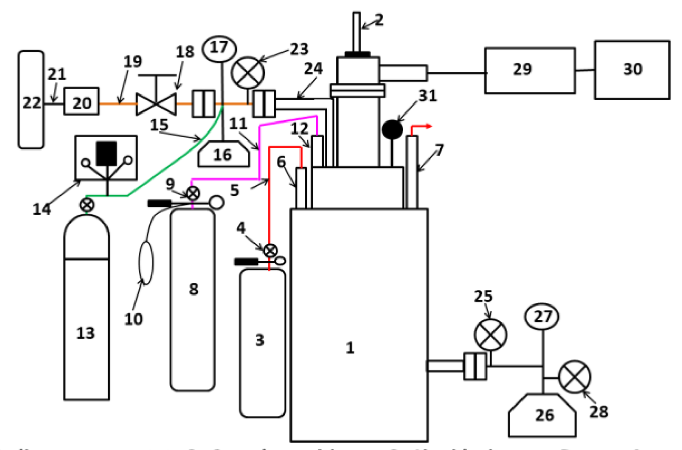

1: Indigenous cryostat; 2: Sample positioner, 3: Liquid nitrogen Dewar, 4: Ball valve, 5: Bare cryogenic transfer line, 6: LN2 filling line, 7: LN2 vent line, 8: Liquid Helium Dewar, 9: Ball valve, 10: Pressurization gas balloon, 11: Flexible cryogenic transfer line, 12: LHe filling line, 13: Helium cylinder, 14: Regulator, 15: Gas charging pipe, 16: Turbomolecular vacuum pump, 17: Pirani gauge, 18: Butterfly Valve, 19: Gaseous helium flow line, 20: Flow meter, 21: Pipe, 22: Central helium storage gas bag, 23: Ball valve, 24: Helium recovery connector, 25: Ball valve, 26: Turbomolecular vacuum pump, 27: Pirani gauge, 28: Ball valve, 29: Temperature controller, 30: PC, 31: Safety valve

Schematics of experimental facility

Photographic view of experimental facility

Experimental procedures and instrumentations are explained in references [2, 3]

ARTIFICIAL NEURAL NETWORK ANALYSIS

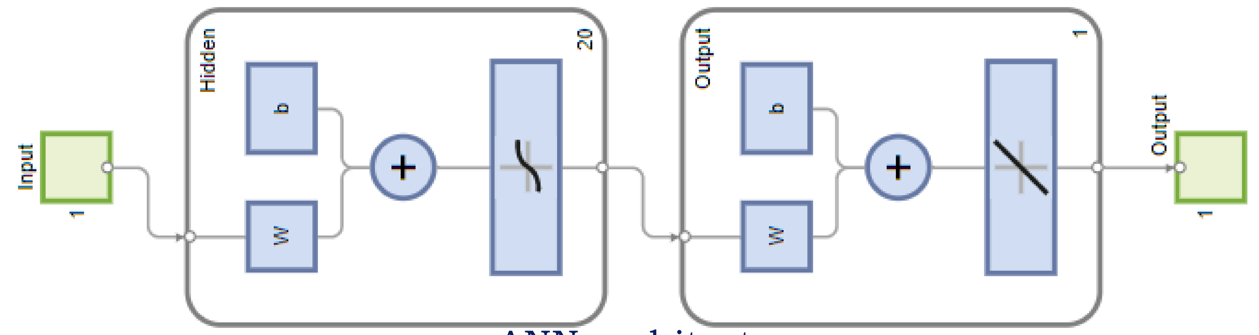

ANN architecture

Mathematical background behind ANN analysis is explained in reference [4,5]

Resistance of sensor for different back prop schemes

Temperature of Cernox (K)	Resistance of the sensor (Ohm)											
	Experimental	Backpropagation schemes										
		h	b	a	j	k	c	d	e	i	g	f
5.0002	1.6213	1.6182	1.6196	3.9607	2.538147	1.688845	1.766439	1.226913	1.327035	-1.77764	52.87454	-486.328
7.5003	1.6478	1.6534	1.6522	3.3452	2.536305	1.651384	1.542669	1.481158	1.612913	1.718693	9.622228	-584.474
10.0069	1.7048	1.6970	1.6964	2.7384	2.531951	1.68979	1.493163	1.714416	1.820719	3.403773	-13.3735	-642.018
20.0664	3.4469	3.4488	3.4490	-8.1268	2.322648	4.113537	4.392768	4.806477	4.190243	4.892477	-46.6204	-611.665
30.0586	10.0562	10.0516	10.0473	-9.6502	-1.21524	8.399953	9.268266	8.929822	8.442757	7.613098	-40.9887	-518.808
40.0324	22.5141	22.5152	22.5199	42.5779	28.11533	25.15788	24.47031	23.32824	23.71582	24.23483	104.1062	-348.663
50.0425	39.507	39.4993	39.5039	44.12678	42.13301	37.45446	37.96966	40.00731	38.61288	38.6007	67.49306	-158.505
60.039	59.139	59.1471	59.1432	36.31418	43.89693	58.53241	58.41347	57.80466	58.95191	57.3889	-7.43192	78.5873
70.0131	80.109	80.1126	80.1132	96.69770	93.77252	82.51254	82.67485	83.06659	82.4038	84.4353	108.4219	224.435
80.0266	101.738	101.732	101.733	115.1899	96.25908	100.2234	99.68783	99.56504	99.10524	98.18898	133.1208	392.106
90.0026	123.428	123.423	123.4216	102.9348	122.9382	123.1959	123.2356	123.4231	124.6953	123.5633	113.3866	687.375
100.013	145.152	145.143	145.1461	149.6863	137.1479	146.8687	147.1205	147.156	145.3927	148.8479	125.868	859.949
110.019	166.732	166.732	166.7312	172.0965	175.0475	164.4996	164.5075	164.0825	165.5599	163.7379	148.0222	843.710
120.003	188.074	188.087	188.0869	184.6880	183.6935	189.6067	189.473	190.0268	188.4927	189.3254	206.4416	536.320
150.006	251.45	251.458	251.4575	253.3896	255.1373	253.2255	253.2809	253.5051	253.7618	254.0197	254.4035	11.2000
200.01	354.98	354.998	354.9984	356.9694	356.9965	354.0523	354.3984	354.075	355.0209	354.3288	346.4531	-218.981
250.006	456.6	456.599	456.6011	450.6370	447.6331	454.1486	455.9898	454.2251	455.8668	454.088	455.7446	618.434
300.326	558.67	558.848	558.9746	640.1824	538.0993	566.6629	565.404	557.4475	567.4462	549.4322	487.8436	489.128

Resistance, sensitivity and dimensionless sensitivity of sensors from 5 K to 300 K

Temperature of Cernox (K)	Resistance (Ohm)	Sensitivity	Dimensionless sensitivity
5.0002	1.6213	0.008547009	0.026359558
7.5003	1.6478	0.015267176	0.069491684
10.0069	1.7048	0.03125	0.183432441
15.0145	2.1356	0.165482234	1.163435566
20.0664	3.4469	0.368522073	2.145380291
25.046	5.9881	0.664939551	2.78119537
30.0586	10.0562	0.973891925	2.911022832
35.0399	15.6153	1.254293263	2.814567155
40.0324	22.5141	1.467817896	2.609932138
45.0515	30.587	1.589648799	2.341388918
50.0425	39.507	1.926701571	2.440503287
55.0123	49.025	1.979752531	2.22153473
60.039	59.139	2.009512485	2.040094017
65.0201	69.508	2.06185567	1.928728518
70.0131	80.109	2.201166181	1.923759726
75.0037	90.85	2.04610951	1.689221617

Temperature of Cernox (K)	Resistance (Ohm)	Sensitivity	Dimensionless sensitivity
80.0266	101.738	2.115987461	1.664425113
85.0308	112.607	2.166377816	1.63585602
90.0026	123.428	2.422997947	1.766828556
95.0295	134.337	2.142857143	1.515849266
100.013	145.152	2.178649237	1.501138435
105.002	155.919	2.19047619	1.475153002
110.019	166.732	2.075	1.369199824
120.003	188.074	1.789473684	1.14179637
125.009	198.742	1.848484848	1.162699593
150.006	251.45	2	1.193127858
175.006	303.39	1.428571429	0.824050138
200.01	354.98	2.222222222	1.25208932
225.01	406.12	1.891891892	1.048199041
250.006	456.6	2.5	1.368845817
275.004	506.68	2.727272727	1.480245735
300.326	558.67	0.785498489	0.422262909

Mathematical background behind computation of sensitivity & dimensionless sensitivity are explained in references [1,6]

RESULTS

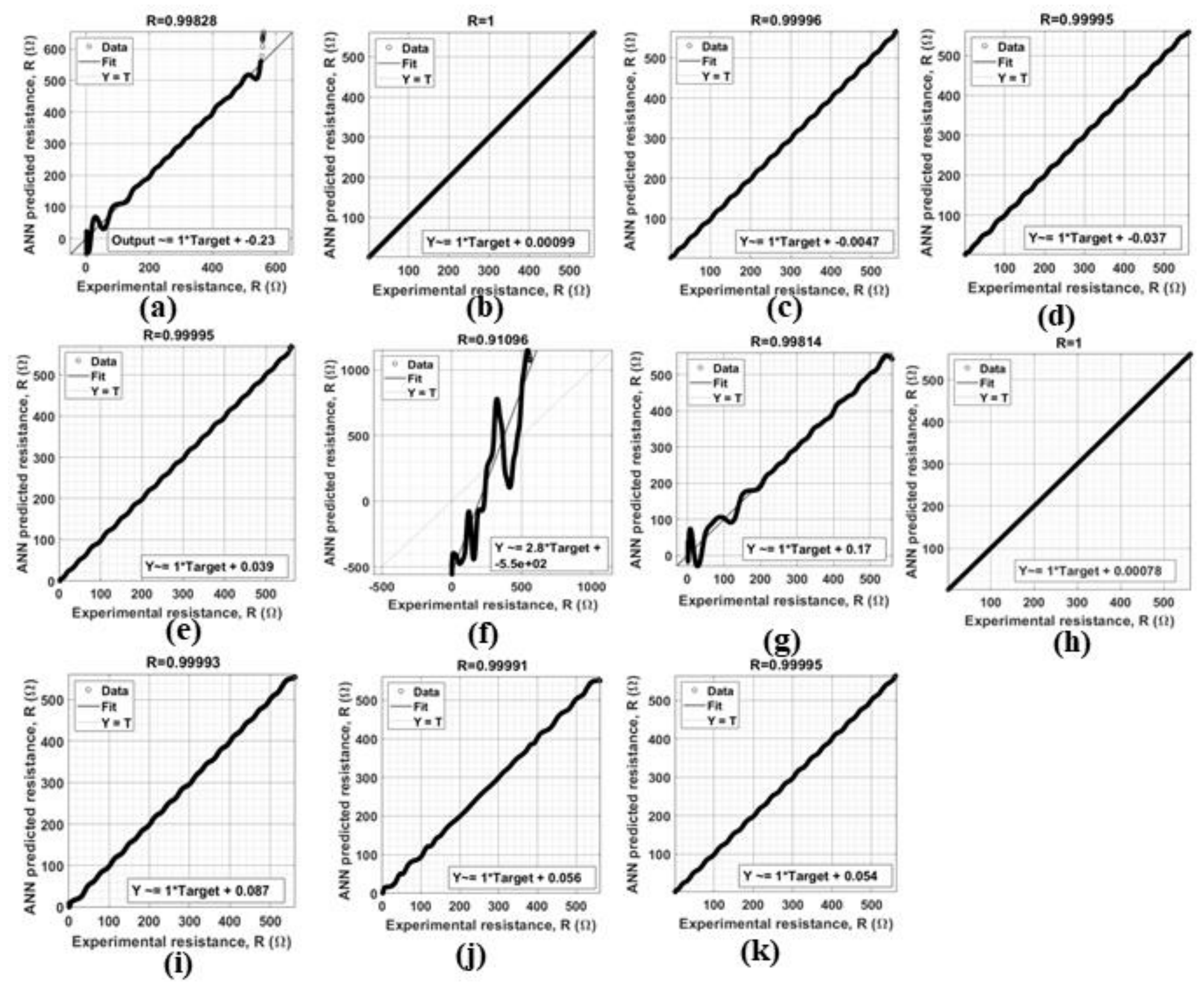

Regression plots of different backpropagation schemes

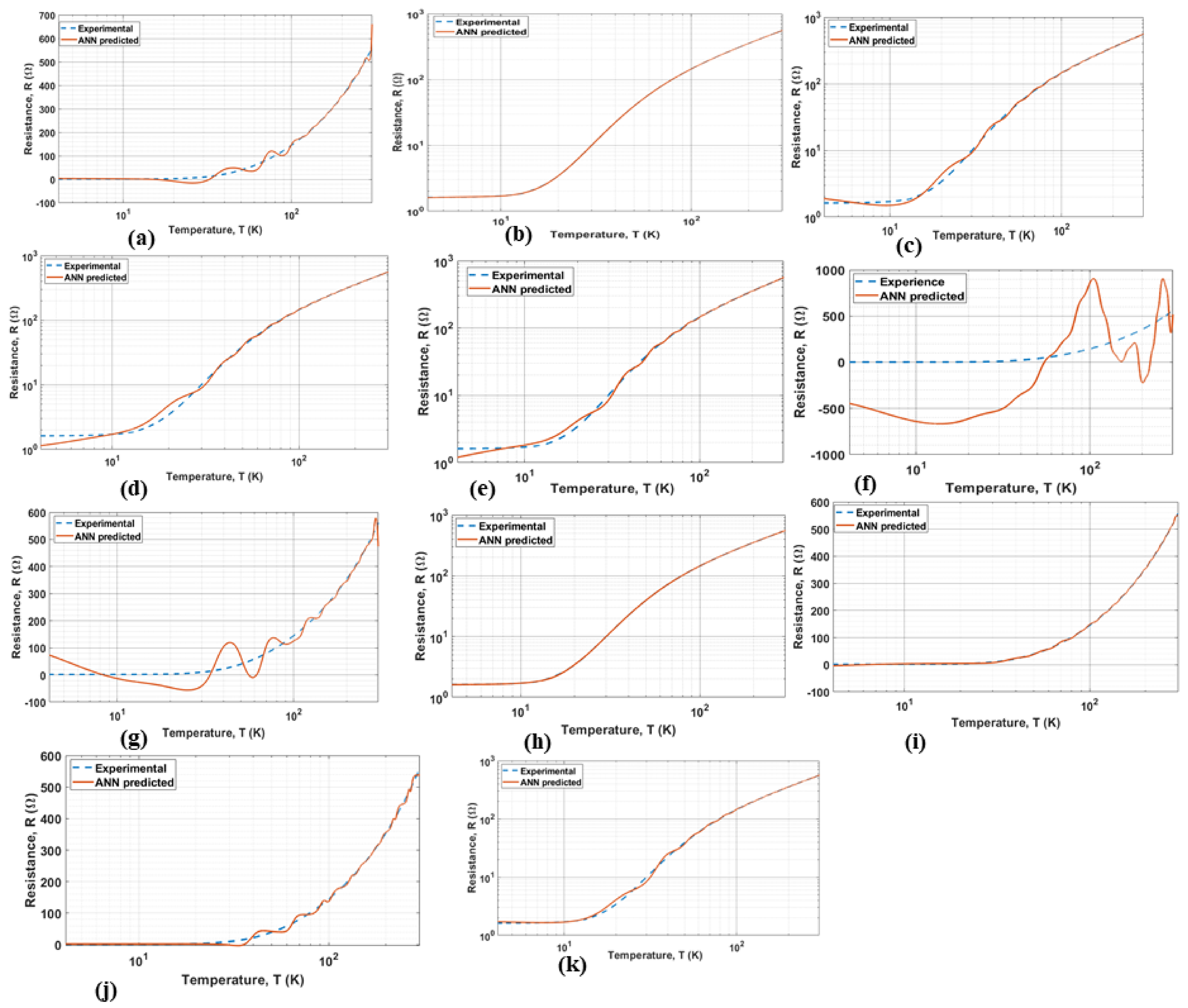

Comparison of ANN results Vs Experimental results

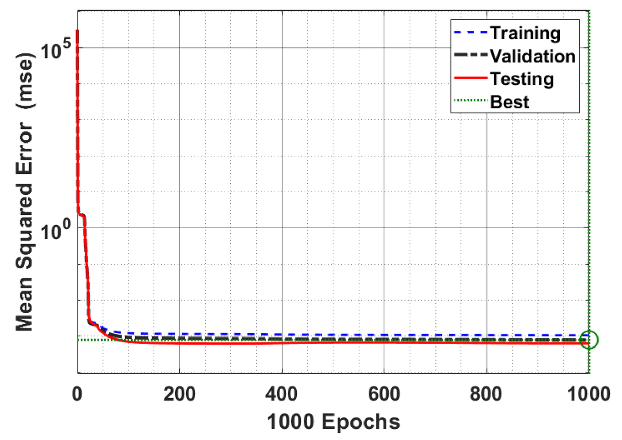

Performance plot of LM scheme

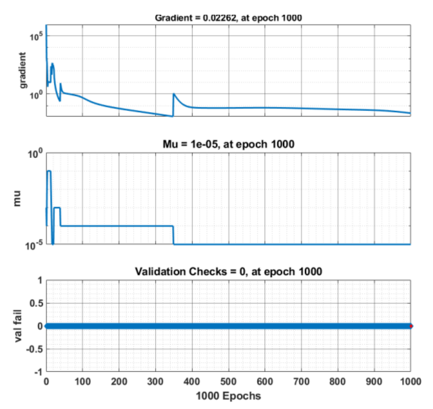

Training state plot

BFGS quasi-Newton backpropagation (a) Bayesian regularization backpropagation (b) Scaled conjugate gradient backpropagation (c) Conjugate gradient backpropagation with Fletcher-Reeves updates (d) Conjugate gradient backpropagation with Polak-Ribiére updates (e) Gradient descent with momentum backpropagation (f) Gradient descent with momentum and adaptive learning rate backpropagation (g) Levenberg-Marquardt backpropagation (h) One-step secant backpropagation (i) Resilient backpropagation (j), Scaled conjugate gradient backpropagation (k).

Details available in reference [4, 5]

CONCLUSIONS

- ✓ An indigenous cryostat have been developed and successfully tested with earlier temperature calibration test rig.
- ✓ Different varieties of resistance sensors have been calibrated from 4.2 K to 300 K and supplied to ISRO for use with launch vehicles.
- ✓ The sensitivity and dimensionless sensitivity of sensors have been computed numerically from experimental data.
- ✓ Artificial neural network has been implemented to fit the relation between resistance vs temperature.
- ✓ Different back propagation algorithms are implemented to establish relation between resistance and temperature. **Scaled conjugate gradient back propagation scheme and Levenberg-Marquardt back propagation schemes** are in an **excellent agreement** with **experimental values** over other selected back propagation schemes.
- ✓ The **developed sensors** are of **excellent sensitivity and accuracy** from cryogenic temperature (4.2 K) to ambient temperature (300 K).

REFERENCES

[1] Re-entry of Cryogenic Upper Stage of LVM3 M4, Vol. 19, The Aeronautical Society of India, E-news, 2024.

[2] Behera, U., Panda, D., Suma M.N., & Suresh, T. (2024). Development of an Indigenous Cryogenic Temperature Sensors Calibration Facility for Cryogenic and Semicryogenic Rocket Engines. In Proceedings of the International Conference on Advances in Aerospace and Energy Systems (April 04-06, 2024), Liquid Propulsion Systems Centre, Valiamala, ISRO, India.

[3] https://www.lakeshore.com/

[4] Kumar, Manoj, Debashis Panda, Suraj K. Behera, and Ranjit K. Sahoo. "Experimental investigation and performance prediction of a cryogenic turboexpander using artificial intelligence techniques." Applied thermal engineering 162 (2019): 114273

[5] https://in.mathworks.com/

[6] S.S. Courts, and B.R. Courts, "Stability of Cernox® temperature sensors stored at room temperature over a 29-year period". Cryogenics, 129, 103616, 2023